

# MEASURABLY STRONGER EXPLANATION RELIABILITY VIA MODEL CANONIZATION

Franz Motzkus      Leander Weber      Sebastian Lapuschkin

Department of Artificial Intelligence, Fraunhofer Heinrich Hertz Institute, 10587 Berlin, Germany

## ABSTRACT

While rule-based attribution methods have proven useful for providing local explanations for Deep Neural Networks, explaining modern and more varied network architectures yields new challenges in generating trustworthy explanations, since the established rule sets might not be sufficient or applicable to novel network structures. As an elegant solution to the above issue, *network canonization* has recently been introduced. This procedure leverages the implementation-dependency of rule-based attributions and restructures a model into a functionally identical equivalent of alternative design to which established attribution rules can be applied. However, the idea of canonization and its usefulness have so far only been explored qualitatively. In this work, we quantitatively verify the beneficial effects of network canonization to rule-based attributions on VGG-16 and ResNet18 models with BatchNorm layers and thus extend the current best practices for obtaining reliable neural network explanations.

## 1. INTRODUCTION

In recent years, the field of eXplainable Artificial Intelligence (XAI) has shifted into focus, with the objective to solve the "black-box"-problem inherent to many (deep) machine learning predictors in order to better understand the reasoning of these models and consequently increase trust in them. Current work from the field has highlighted the usefulness of contemporary XAI approaches for understanding and improving models and datasets in various application scenarios [1].

Many contemporary explainability methods yield so-called attribution maps, i.e., per-input-dimension indicators of how (much) a model, e.g., a Deep Neural Network (DNN), has used the value of a particular input unit during inference [2, 3], or whether the model is sensitive to its change [4, 5]. This information can be obtained either via perturbation-based approaches treating the model as a black-box [6], based on the gradient [7, 8], or with techniques applying modified backpropagation through the model [2, 3]. While (modified) backpropagation-based methods are popular choices for large-scale XAI experiments and practitioners, e.g., due to their efficiency and expressivity, rule-based variants such

as Layer-wise Relevance Propagation or Excitation Back-propagation are known to not be implementation invariant [9]: Rule-based methods assign dedicated backpropagation "rules" to different parts of a neural network, allowing for individual treatment of specific layers attuned to their function within the model [10]. That is, with DNNs representing complex mathematical functions in a structured manner via layers, a different expression of the very same function via an alternative or completely new network architecture may lead to different — or in the worst case even misrepresentative — explanation outcomes. Furthermore, the continuous evolution of neural network architectures requires rule-based methods to regularly adapt to newly introduced network elements such as BatchNorm (BN) [11] layers or skip connections in ResNets [12].

In awareness to these issues, *neural network canonization* has been introduced in previous work [13, 14] and constitutes an elegant solution for transforming a variety of highly specialized neural network elements into canonical and well-understood, yet functionally equivalent network architectures for improved model explainability, where established rules are easily applicable. Thereby, network canonization has the potential for improving a model's architecture (w.r.t. its original design) to *fix problems* in an explainability context, and thus *increase the potential* for model trustworthiness without affecting its functionality. Existing work [15] describes canonization as a required step for reliable results, and, as a consequence, the authors of XAI software even build such model processors into their toolkits [16]. Assessments of network canonization on visualized attribution maps [13, 14] exist on a qualitative level. However, to the best of our knowledge, there is no single study dedicated to the *quantification* of the beneficial effects of canonization on neural network explanations.

In this work, we dedicate efforts to the quantification and numerical verification of the benefits of canonization on two popular DNN architectures (VGG-16 [17] and ResNet18 [12] models, in representation of similar architectures) on data from the ILSVRC2012 [18] benchmark dataset. In particular, with a focus on variants of the popular Layer-wise Relevance Propagation [2] technique and gradient-based attribution methods, we canonically extend the work of [13, 14] by measurably demonstrating — at hand of experiments of attribution-guided input perturbation [19] and object local-

This work was supported by the European Union's Horizon 2020 research and innovation programme (EU Horizon 2020) as grant [iToBoS (965221)]. ✉ sebastian.lapuschkin@hhi.fraunhofer.de

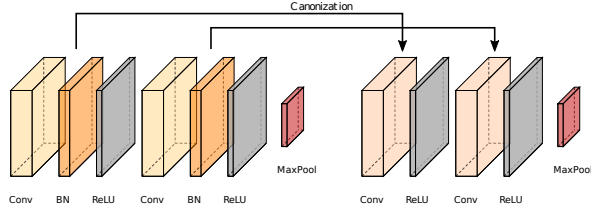


**Fig. 1.** Exemplary canonization of a VGG-16 model segment with BN layers. As the BN is applied before the activation, the parameters of the convolution and the BN are fused to build a new convolutional layer. The BN layer is then omitted.

ization using annotated ground truth bounding boxes [10] — that model canonization is a critical factor for improving the quality and faithfulness of local explanations in rule-based approaches.

## 2. METHODS

### 2.1. Network Canonization

BatchNorm (BN) layers [11] have been shown to be effective building blocks for improving and accelerating neural network training. By eliminating the internal covariate shift in the activations, they stabilize the distribution of intermediate representations and improve the gradient flow through the network, mitigating issues such as gradient shattering or -explosion [11]. In some modified backpropagation methods, such as Layer-wise Relevance Propagation (LRP), it is not inherently clear how to adequately propagate attribution scores through BN layers. An elegant solution for avoiding this issue altogether is to apply model canonization to these layers [13, 14, 20]. That is, a model (or parts thereof) is restructured in such a way that the result is functionally equivalent in terms of inference behavior for all possible input samples, but only contains layer types supported by well-understood attribution propagation rules. For this purpose, BN layers are commonly resolved by merging their parameters with an adjacent linear (i.e., convolutional or fully-connected) layer [14, 20] into a single and functionally equivalent linear layer with fused parameters, replacing both original layers.

A schematic example for canonization is given in Figure 1. The relative positioning of the BN and linear layers, as well as the ReLU nonlinearity, determines which linear layer to update with the BN parameters. We evaluate attributions for pre-trained VGG-16 [17] and ResNet18 [12] models in our experiments (Section 3), which both contain segments of triples of *Convolution*  $\rightarrow$  *BN*  $\rightarrow$  *ReLU*.

Let a convolutional layer  $y_{\text{conv}} = w_{\text{conv}} \cdot x + b_{\text{conv}}$ , with weight and bias parameters  $w_{\text{conv}}$ ,  $b_{\text{conv}}$ , be followed by a BN layer  $y_{\text{bn}} = w_{\text{bn}} \cdot \frac{y_{\text{conv}} - \mu_{\text{bn}}}{s_{\text{bn}}} - b_{\text{bn}}$ , with  $s_{\text{bn}} = \sqrt{\sigma_{\text{bn}}^2 + \varepsilon}$ . Here,  $\mu_{\text{bn}}$  is the running mean and  $\sigma_{\text{bn}}^2$  the running variance<sup>1</sup>,  $w_{\text{bn}}$ ,

<sup>1</sup> $\mu_{\text{bn}}$  and  $\sigma_{\text{bn}}^2$  parameters are fixed after training [11].

$b_{\text{bn}}$  are learnable parameters, and  $\varepsilon$  a small stabilizing constant. Following the derivations in [20], the parameters  $w_c$  and  $b_c$  of the merged layer  $y_{\text{bn}} = w_c \cdot x + b_c$  are then obtained as

$$w_c = \frac{w_{\text{bn}}}{s_{\text{bn}}} \cdot w_{\text{conv}}; \quad b_c = \frac{w_{\text{bn}}}{s_{\text{bn}}} \cdot (b_{\text{conv}} - \mu_{\text{bn}}) + b_{\text{bn}}. \quad (1)$$

We restrict our considerations to the above case, as we employ VGG- and ResNet-type architectures in our experiments. Note, however, that other architectures may require different approaches for canonization [20].

### 2.2. Quantifying the Quality of Explanations

We aim to evaluate the effects of model canonization on explanations not only qualitatively but also quantitatively. Therefore, for our experiments, we selected two measures that quantify two different major properties of explanations: *Attribution Localization* [10] measures the inside-total ratio  $\mu$  of the sum of positive attributions inside the ground truth bounding box(es) ( $R_{\text{in}}^+$ ) vs. the sum of all positive attributions ( $R_{\text{total}}^+$ ) w.r.t. the target label:

$$\mu = \frac{R_{\text{in}}^+}{R_{\text{total}}^+} \quad (2)$$

This measure assumes that the model prediction is based on the object within the bounding box (which can safely be assumed in most cases [10]), and it is maximized if all positive attribution quantity for the target class is concentrated within that area. We complement this localization test with *Input Perturbation Testing* [2, 19], which does not require additional ground truth annotations. This measure creates a ranking of input regions by sorting per-region attributions in descending order, and successively perturbs those regions in that order. After each perturbation, the model is evaluated on the perturbed data sample. The effect of the perturbation on the model w.r.t. the original sample is recorded as

$$x^{(k)} = g(x^{(k-1)}, r) \\ \text{IP}(x, k) = f(x^{(0)}) - f(x^{(k)}), \quad (3)$$

where  $g$  is a function applying the  $k$ th perturbation step on  $x^{(k-1)}$  according to the attribution-ranked regions  $r$  that correspond to the input sample  $x$ . Then,  $x^{(k)}$  is the sample after  $k$  perturbation steps and  $x^{(0)} = x$ . This measure is maximized if the regions ranked first in  $r$  according to the attribution map lead to the sharpest decrease in the output probability of the target class, and therefore measures the faithfulness of the explaining attribution map to the prediction function.

In our experiments, we compute and evaluate attributions for a sample’s true class by perturbing single-pixel regions. We replace perturbed pixels with values drawn from a uniform distribution of all possible pixel values.

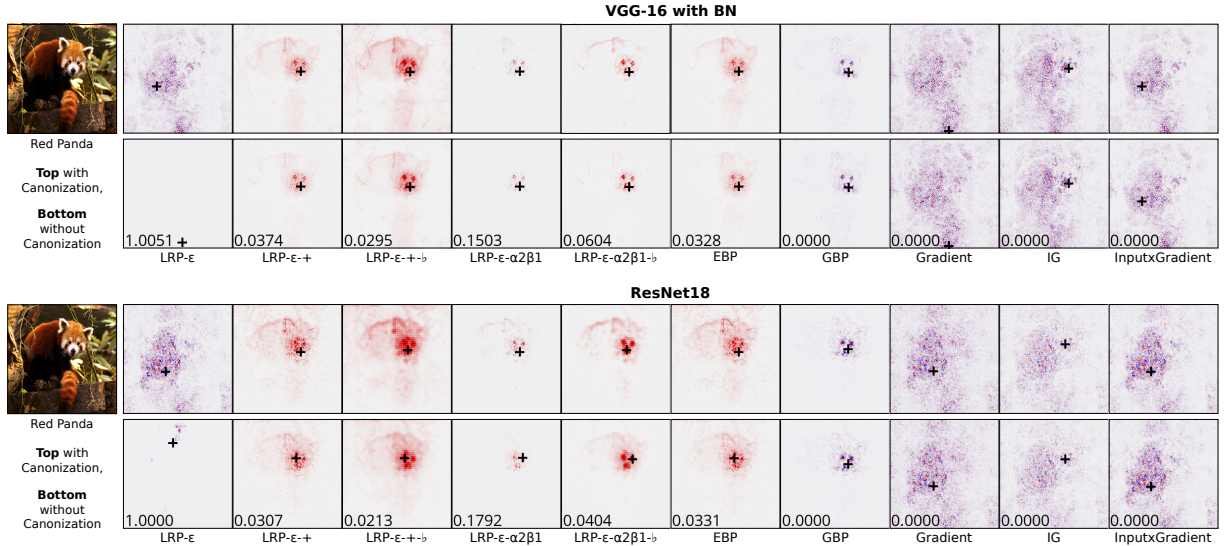


**Fig. 2.** Explanations for VGG-16 (*top*) and ResNet18 (*bottom*) with and without network canonization in comparison for multiple attribution methods. Black crosses localize the highest attributed value per map. Red pixels receive positive attribution values, blue pixels receive negative scores. The cosine distances between both explanations from the original and the canonized model are noted in the bottom left corner of each attribution map without model canonization. Other than gradient-based approaches, rule-based attribution approaches are affected by structural changes resulting in an otherwise equivalent model.

### 3. RESULTS AND DISCUSSION

In this section, the qualitative effects of canonization are evaluated with a visual inspection of the explanations for single samples, while the quantitative effects are measured via the two methods introduced in Section 2.2. For our results, two commonly used model architectures are tested. We evaluate a VGG-16 model with BN after each convolutional layer and a ResNet18 model, both with pre-trained weights from the Pytorchmodel zoo, on a subset of samples derived from 20 randomly picked ILSVRC2012 [18] classes<sup>2</sup>, counting 9758 samples with ground truth bounding boxes in total. We compute attributions for variants of LRP [2] (cf. [10] for details), Excitation Backpropagation (EBP) [21], Guided Backpropagation (GBP) [22], Input×Gradient (I×G) [23], Integrated Gradients (IG) [8] and the gradient itself using *zennit* [16] and its *Canonizer* implementations for comparison.

An example of the explanations for the canonized and non-canonized models can be seen in Figure 2, for VGG-16 (*Top*) and ResNet18 (*Bottom*). As expected, attributions of Gradient, IG, and I×G do not visually change with canonization, which is further confirmed by the cosine-difference between attributions, since neither gradients nor inputs are altered by canonization (although slight numerical differences may arise in practice). For the modified backpropagation methods, however, differing results can be observed: GBP shows no difference between canonized and non-canonized

models, as it only alters the backpropagation through ReLU activations [22]. But the number of ReLU activations and their placement is not affected by the canonization applied here, so that the equal results are expected. However, EBP and LRP-based methods show significant differences between canonized and non-canonized models: For LRP- $\epsilon$ , a clear advantage can be detected for both canonized models, as the explanations for the non-canonized models do not reflect any recognizable input features. Note that this result strongly differs from our observations for I×G, so that claims of I×G and LRP- $\epsilon$  being equal [23] do not hold here. But for the other LRP configurations, differences are not as obvious (although still visible), and explanations of canonized and non-canonized models show a broad similarity. It seems that, by only relying on a visual inspection, fine-grained comparisons between similar XAI methods cannot be made in general, and the perceived differences can thus not be linked to a statement about a disparity in quality. Therefore, independent and quantitative measures are essential for assessing the effects of canonization.

For this purpose, we employ two quantitative metrics focusing on different aspects of explanation quality. In the localization tests (see Figure 3), explanations of LRP methods and Excitation Backpropagation achieve a higher inside-total ratio  $\mu$  for the canonized models (*Top*: VGG-16, *Bottom*: ResNet18), indicating that these explanations increase focus on the expected (bounding box) area and that canonization is therefore clearly beneficial. Note that the relative improvement in localization score is especially significant for

<sup>2</sup>'airship', 'balloon', 'banana', 'barometer', 'binder', 'bison', 'broccoli', 'electric guitar', 'electric switch', 'freight car', 'go-kart', 'hourglass', 'isopod', 'ladybug', 'red panda', 'reel', 'Shih-Tzu', 'tiger', 'toucan', 'volleyball'

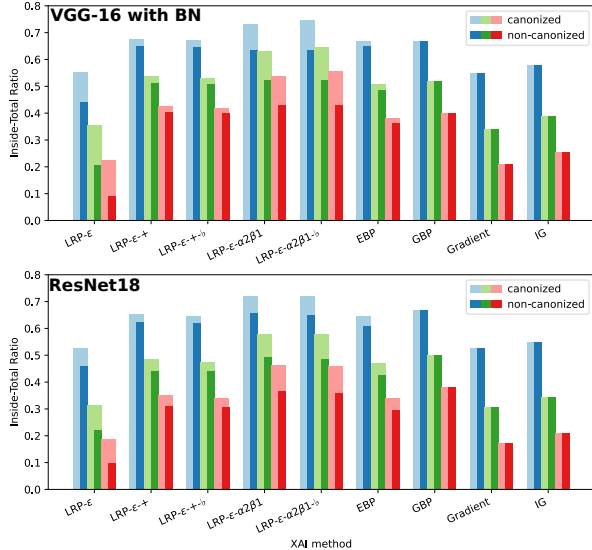


**Fig. 3.** Comparison of the attribution localization scores for the canonized and the non-canonized VGG-16 with BN (*top*) and ResNet18 (*bottom*). Bars show the mean localization scores over all labelled objects from the analyzed ILSVRC2012 subset. Blue bars show the score for *all* objects, while green and red bars show scores for objects with bounding boxes smaller than 50% and 25% of the image size respectively. Different values are evaluated to ensure result independence from bounding box size, see [10]. Color intensity indicates canonization status.

the smaller bounding boxes where generally there is a much higher potential for attributions to be off-target. For the other explanation methods, no changes in localization scores can be observed.

Similarly, the difference in input perturbation test scores between canonized and non-canonized models shown in Figure 4 (*Left*: VGG-16, *Right*: ResNet18) indicate an improvement in modified backpropagation explanation faithfulness to model decisions with canonization. In accordance with our qualitative findings (cf. Figure 2), for both models, the input perturbation scores change the most for LRP- $\epsilon$ . Since LRP- $\epsilon$  favors sensitivity to model parameters over clarity of visual representation, canonization seems to improve explanations by correctly incorporating model parameters for explaining the model decisions. Surprisingly, for LRP- $\epsilon$ - $\alpha 2\beta 1$ - $b$  the score for the attributions of the canonized VGG-16 is worse, while for the ResNet18 canonization improves the attribution faithfulness. The  $b$ -rule employed here introduces imprecision by smoothing in favor of readability. Thus, the effect of the  $b$ -rule is especially noticable when, as in our case, only single pixels are perturbed at a time, as opposed to larger regions. For LRP- $\epsilon$ - $\alpha 2\beta 1$ - $b$ , the sensitivity to correct parameter incorporation is therefore decreased, leading to diverging results between model architectures. Despite showing visual

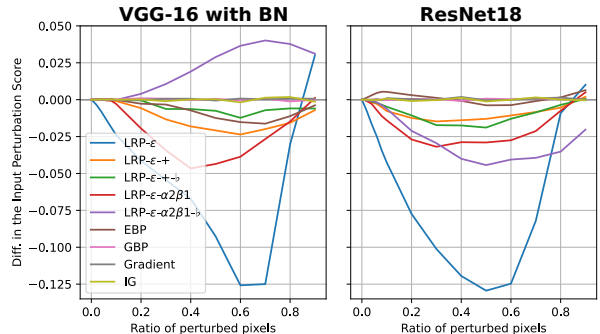


**Fig. 4.** Differences in the input perturbation scores between the canonized and the non-canonized model. Scores have been obtained for the VGG-16 (*left*) and the ResNet18 (*right*) models on the ILSVRC2012 subset, using uniform sampling for replacing pixels. Negative values are associated with increased faithfulness score of the canonized model.

changes in Figure 2 and improved localization scores in Figure 3, the effect of canonization on EBP explanations seems ambiguous in terms of faithfulness. In contrast, the difference for gradient-based methods, as well as for GBP, is close to zero for both VGG-16 and ResNet18, as can be expected due to the corresponding explanations (and gradients) not being affected by canonization. Note that — opposed to the localization scores and qualitative results — the difference is not exactly zero as per the random choice of replacement values in the perturbation function inducing small variations between canonized and non-canonized models’ evaluation.

## 4. CONCLUSION

We confirmed that canonization of BN-layers does not affect gradient-based explanation methods, but can lead to significant improvements for modified backpropagation methods without specified rules for BN layers. While visual differences may be apparent, we observed that qualitative evaluations are generally not sufficient for determining whether canonization leads to better explanations. Utilizing two quantitative measures, testing the *localization* and *faithfulness* of explanations, respectively, we found that canonization significantly improves both properties in general — given that the explanation method is affected by canonization at all. In doing so, canonization can provide attributions that reliably represent a model’s behavior, playing an important role in ensuring model trustworthiness via explanations.

## 5. REFERENCES

[1] Wojciech Samek, Grégoire Montavon, Sebastian Lapuschkin, Christopher J Anders, and Klaus-Robert Müller, “Explaining deep neural networks and beyond:

- A review of methods and applications,” *Proc. IEEE*, vol. 109, no. 3, pp. 247–278, 2021.
- [2] Sebastian Bach, Alexander Binder, Grégoire Montavon, Frederick Klauschen, Klaus-Robert Müller, and Wojciech Samek, “On pixel-wise explanations for non-linear classifier decisions by layer-wise relevance propagation,” *PLOS ONE*, vol. 10, no. 7, pp. 1–46, 07 2015.
- [3] Avanti Shrikumar, Peyton Greenside, and Anshul Kundaje, “Learning important features through propagating activation differences,” in *Proc. ICML. 2017*, vol. 70 of *Proc. MLR*, pp. 3145–3153, PMLR.
- [4] Niels JS Morch, Ulrik Kjems, Lars Kai Hansen, Claus Svarer, Ian Law, Benny Lautrup, Steve Strother, and Kelly Rehm, “Visualization of neural networks using saliency maps,” in *Proc. ICNN. IEEE, 1995*, vol. 4, pp. 2085–2090.
- [5] David Baehrens, Timon Schroeter, Stefan Harmeling, Motoaki Kawanabe, Katja Hansen, and Klaus-Robert Müller, “How to explain individual classification decisions,” *JMLR*, vol. 11, pp. 1803–1831, 2010.
- [6] Marco Tulio Ribeiro, Sameer Singh, and Carlos Guestrin, ““Why should i trust you?” explaining the predictions of any classifier,” in *Proc. ACM SIGKDD, 2016*, pp. 1135–1144.
- [7] Karen Simonyan, Andrea Vedaldi, and Andrew Zisserman, “Deep inside convolutional networks: Visualising image classification models and saliency maps,” in *Proc. ICLR, 2014*.
- [8] Mukund Sundararajan, Ankur Taly, and Qiqi Yan, “Axiomatic attribution for deep networks,” in *Proc. ICML, 2017*, pp. 3319–3328.
- [9] Grégoire Montavon, “Gradient-based vs. propagation-based explanations: An axiomatic comparison,” in *Explainable AI: Interpreting, Explaining and Visualizing Deep Learning*, vol. 11700 of *Lecture Notes in Computer Science*, pp. 253–265. Springer, 2019.
- [10] Maximilian Kohlbrenner, Alexander Bauer, Shinichi Nakajima, Alexander Binder, Wojciech Samek, and Sebastian Lapuschkin, “Towards best practice in explaining neural network decisions with lrp,” in *IJCNN, 2020*, pp. 1–7.
- [11] Sergey Ioffe and Christian Szegedy, “Batch normalization: Accelerating deep network training by reducing internal covariate shift,” in *Proc. ICML. 2015*, vol. 37 of *JMLR Workshop Conf. Proc.*, pp. 448–456, JMLR.org.
- [12] Kaiming He, Xiangyu Zhang, Shaoqing Ren, and Jian Sun, “Deep residual learning for image recognition,” in *CVPR, 2016*, pp. 770–778, IEEE Computer Society.
- [13] Lucas Y. W. Hui and Alexander Binder, “Batchnorm decomposition for deep neural network interpretation,” in *ADCI, Cham, 2019*, pp. 280–291, Springer International Publishing.
- [14] Mathilde Guillemot, Catherine Heusele, Rodolphe Korch, Sylvianne Schnebert, and Liming Chen, “Breaking batch normalization for better explainability of deep neural networks through layer-wise relevance propagation,” *arXiv preprint arXiv:2002.11018*, 2020.
- [15] Seul-Ki Yeom, Philipp Seegerer, Sebastian Lapuschkin, Alexander Binder, Simon Wiedemann, Klaus-Robert Müller, and Wojciech Samek, “Pruning by explaining: A novel criterion for deep neural network pruning,” *Pattern Recognition*, vol. 115, pp. 107899, 2021.
- [16] Christopher J. Anders, David Neumann, Wojciech Samek, Klaus-Robert Müller, and Sebastian Lapuschkin, “Software for dataset-wide XAI: from local explanations to global insights with zennit, corelay, and virelay,” *arXiv preprint arXiv:2106.13200*, 2021.
- [17] Karen Simonyan and Andrew Zisserman, “Very deep convolutional networks for large-scale image recognition,” in *Proc. ICLR, 2015*.
- [18] Olga Russakovsky, Jia Deng, Hao Su, Jonathan Krause, Sanjeev Satheesh, Sean Ma, Zhiheng Huang, Andrej Karpathy, Aditya Khosla, Michael S. Bernstein, Alexander C. Berg, and Li Fei-Fei, “Imagenet large scale visual recognition challenge,” *IJCV*, vol. 115, no. 3, pp. 211–252, 2015.
- [19] Wojciech Samek, Alexander Binder, Grégoire Montavon, Sebastian Lapuschkin, and Klaus-Robert Müller, “Evaluating the visualization of what a deep neural network has learned,” *IEEE Trans. Neural Networks Learn. Syst.*, vol. 28, no. 11, pp. 2660–2673, 2017.
- [20] Alexander Binder, “Notes on canonization for resnets and densenets,” [https://github.com/AlexBinder/LRP\\_Pytorch\\_Resnets\\_Densenet/blob/master/canonization\\_doc.pdf](https://github.com/AlexBinder/LRP_Pytorch_Resnets_Densenet/blob/master/canonization_doc.pdf), 2020.
- [21] Jianming Zhang, Sarah Adel Bargal, Zhe Lin, Jonathan Brandt, Xiaohui Shen, and Stan Sclaroff, “Top-down neural attention by excitation backprop,” *International Journal of Computer Vision*, vol. 126, no. 10, pp. 1084–1102, 2018.
- [22] Jost Tobias Springenberg, Alexey Dosovitskiy, Thomas Brox, and Martin A. Riedmiller, “Striving for simplicity: The all convolutional net,” in *Proc. ICLR, 2015*.
- [23] Avanti Shrikumar, Peyton Greenside, Anna Shcherbina, and Anshul Kundaje, “Not just a black box: Learning important features through propagating activation differences,” *arXiv preprint arXiv:1605.01713*, 2016.